Proceedings Paper:
Sorour, M, Elgeneidy, K, Hanheide, M et al. (2020) Enhancing Grasp Pose Computation in Gripper Workspace Spheres. In: Proceedings of the 2020 IEEE International Conference on Robotics and Automation (ICRA). 2020 IEEE International Conference on Robotics and Automation (ICRA), 31 May - 31 Aug 2020, Paris, France. IEEE, pp. 1539-1545. ISBN: 978-1-7281-7396-2. ISSN: 1050-4729. EISSN: 2577-087X.

https://doi.org/10.1109/icra40945.2020.9196863

Enhancing Grasp Pose Computation in Gripper Workspace Spheres

M. Sorour, K. Elgeneidy, M. Hanheide, M. Abdalmjed, A. Srinivasan, and G. Neumann

***Abstract*— In this paper, enhancement to the novel grasp planning algorithm based on gripper workspace spheres is presented. Our development requires a registered point cloud of the target from different views, assuming no prior knowledge of the object, nor any of its properties. This work features a new set of metrics for grasp pose candidates evaluation, as well as exploring the impact of high object sampling on grasp success rates. In addition to gripper position sampling, we now perform orientation sampling about the x, y, and z-axes, hence the grasping algorithm no longer require object orientation estimation. Successful experiments have been conducted on a simple jaw gripper (Franka Panda gripper) as well as a complex, high Degree of Freedom (DoF) hand (Allegro hand) as a proof of its versatility. Higher grasp success rates of 76% and 85.5% respectively has been reported by real world experiments.**

***Index Terms*— grasping, manipulation.**

I. Introduction

Geometric based methods [1]–[4] along side deep learning [5]–[9] can be considered the two most successful approaches in grasp planning problem, specially for unknown objects among others [10]–[13]. On the one hand, deep learning is able to model very complex systems, and has become more affordable thanks to advances in hardware computational power and indeed high grasp success rates has been reported [14]. However, this approach require extensive offline processing and sufficiently large training data sets, and at the moment, versatility to different gripper structures [15] remains a challenge, where most of the available works focus on simple parallel jaw grippers. On the other hand, geometry based approaches generally provide no sacrifice on generality or success rates.

Grasp planning of unknown objects from point cloud data is presented in [1], using geometric information to categorize objects into shape primitives, with predefined strategies for each. Success rate of 82% is achieved. This approach is similar to the pioneering work in [2], [16] with the later employing machine learning in grasp selection. In [17], similar approach is employed, more suitable for generalization, however, only simulations are provided with no real world experiments. In [18], a set of contact points that fulfill certain geometric conditions are computed for unknown objects in point cloud, these are ranked to find the most stable grasp. The algorithm is limited to 2 fingered grippers, and no data regarding grasping success rate is presented.

In [3], object shape reconstruction is performed online from successive image data, their method is general for different kinds of multi-fingered hands, while in [19], fast shape reconstruction algorithm is presented as means of improving grasping algorithms. Other geometric approaches are used to synthesize force balanced grasps as in [15], [20], [21], however the work is mainly focusing on 2 fingered grippers, the same issue can be found in [4], where a grasp planner is designed to fit only a jaw gripper by searching for two parallel line segments in the object image. In [22], the authors presented a grasp planner using single depth image of a non-occluded object. Their work, however, is limited to 2 fingered grippers as well as the geometry based planner in [23]. Recently, the authors in [24] proposed a grasp planner based on similarity metric of local surface features between object and gripper's finger surfaces. Experiments on heap of objects were successfully conducted, however using only a 2 fingered gripper. Similar approach is presented in [25], with rather more freedom to modify gripper shape to match that of the object.

Few authors presented grasping algorithms suitable for different gripper structures. In [26], a two-step cascaded deep networks were used to detect grasping rectangle on objects, the results were applied on 2 grippers, but both are of parallel jaw structure. Grasp success reported was

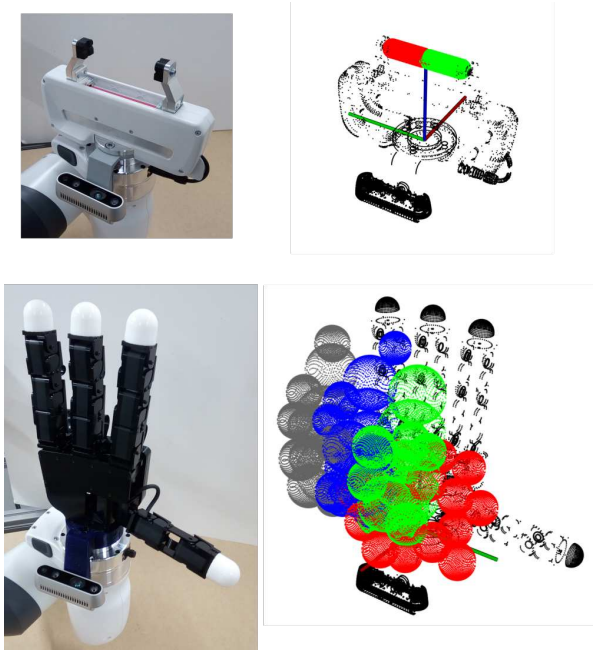

Fig. 1: Gripper workspace spheres (right), for the Franka panda gripper (upper) and the Allegro right hand (lower), featuring 10 spheres per finger with the color code: thumb(red), index(green), middle(blue), and pinky(grey). The real hardware shown to the left, fitted with the Intel Realsense d435 depth camera.

Lincoln Center for Autonomous Systems (L-CAS), School of Computer Science, University of Lincoln, Brayford Pool, LN6 7TS Lincoln, United Kingdom. msorour@lincoln.ac.uk

84% with average per-object trials of 4, which is quite few. In [27], learning based algorithm is developed and applied to a parallel jaw gripper and a 2 DoF prosthetic hand, the latter being controlled in 1 DoF treated as a complex shape parallel jaw. Experiments were focusing on clearing a table and emptying a basket with success rates within 87% to 94%. For single object grasp, a success rate of 92% is reported for a set of 10 objects with only 50 trials in total, which we believe is quite low for evaluation. The success rate drops to 85% using the multi-DoF hand. In [28], a geometry based grasping algorithm is presented, the development includes some empirically tuned parameters, tailored for 2 fingered grippers (grasp planning for 2 contact points), with adaptation for multi-fingered hands. This adaptation, however, limits the performance of complex hands by treating it as 2 fingered. An average success rate of 86% was reported.

In this work, we present further enhancements to the novel grasp planning algorithm previously introduced by the authors in recent work [29], resulting in a boost of the grasp success rate up to 76%, and 85.5% for multi-DoF hand (Allegro hand), and the parallel jaw gripper (Franka panda gripper) respectively. Our algorithm, based on gripper workspace spheres (depicted in Fig. 1), takes an all-around point cloud of the object (by registering 3 partial view point clouds from various poses) as input, and outputs a $6D$ grasp pose. The object bounding box dimensions are computed and sampled into uniformly distributed points in x, y, and z-axes serving as position anchors, where the gripper workspace centroid is placed. At each of these positions, orientation angles about x, y, and z-axes are sampled to provide further orientation sampling, which serves as a new feature in the current development. For each of these position/orientation sample pair, the gripper pose is collision checked against both the object plane (table) as well as the object itself. Various evaluation metrics, newly introduced in this work, are used to give each collision free gripper postures a total score, the one with highest value is then selected for execution.

The contribution of the work presented in this paper is twofold:

- New evaluation metrics: specifically introducing the gripper support regions, which increased the grasp contact area and as such resulted in more stable grasps.
- Exploring higher sampling: with introducing orientation samples in x, y, and z-axes instead of orientation about the object major axis (in previous work). As such we no longer require an estimate of the object orientation, which is both difficult to obtain as well as meaningless for irregular/complex shaped objects.

These contributions had a direct impact on boosting the grasp success rate from 65% to 76%, and 85.5% for the Allegro hand, and the Franka gripper respectively.

The paper is organised as follows: section II provides a summary of the grasping algorithm. Newly developed evaluation metrics are detailed in section III. Experimental results, discussion, and future work are reported in section IV. Conclusions are finally given in section V.

II. Grasping Algorithm

In this section, we briefly describe the grasping algorithm detailed in [29]. Figure 2 shows the coordinate frames of the system components used in this development, namely the camera $\mathcal{F}_c$, end-effector $\mathcal{F}_E$, gripper $\mathcal{F}_g$, object $\mathcal{F}_o$, table $\mathcal{F}_t$ frames, and the arm base $\mathcal{F}_0$ frame. The frames $\mathcal{F}_c$ and $\mathcal{F}_g$ are fixed with respect to the end-effector frame $\mathcal{F}_E$, but are justified, where the object point cloud is obtained in $\mathcal{F}_c$, the gripper point cloud and special ellipsoids are more conveniently developed in $\mathcal{F}_g$. In what follows, matrices and vectors will be designated by bold uppercase and lowercase letters respectively. Point clouds shall be indicated by the $\mathcal{C}$ symbol. Sphere and special ellipsoid clouds with $\mathcal{S}$ and $\mathcal{E}$ respectively, each is a point cloud containing the $3D$ offset point, in addition to the $1D$ radius for a sphere, or the $3D$ principal semi-axes parameters for a special ellipsoid (SE). The left superscript shall indicate the frame of reference.

A. Preface

The grasping algorithm consists of few offline computations, that is done only once, per gripper, where first, the 3D CAD model is used to generate a downsampled gripper point cloud ${}^g\mathcal{C}_g \in \mathbb{R}^{n_g \times 3}$, where n_g is the number of cloud points. Second a set of special ellipsoids are constructed ${}^g\mathcal{E}_g \in \mathbb{R}^{n_e \times 6}$, with n_e denoting the number of gripper special ellipsoids, acting as shape approximation of the gripper as seen in Fig. 3 (d,e). Third, to generate a point cloud (sampling) of the workspace of each finger of the gripper, and fill it with a set of spheres ${}^g\mathcal{S}^f \in \mathbb{R}^{n_{sp} \times 4}$, with $f \in \{2 \dots n_f\}$ denoting the gripper finger index, and n_{sp}, n_f, the number of spheres and fingers respectively.

In this work, we approximate cuboid like shapes using what we call "special ellipsoid", this is a variation of the

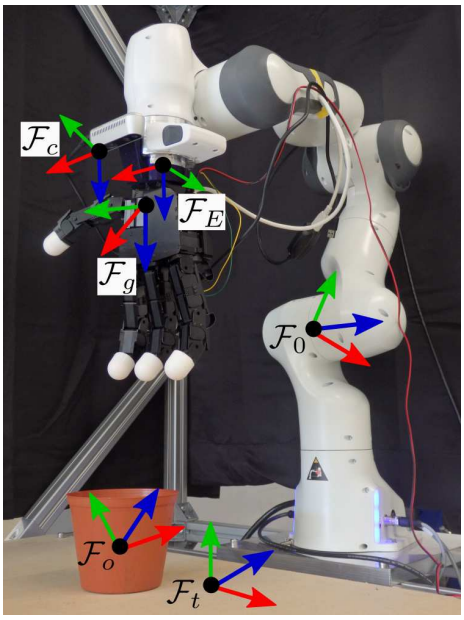

Fig. 2: System frames used in our algorithm.

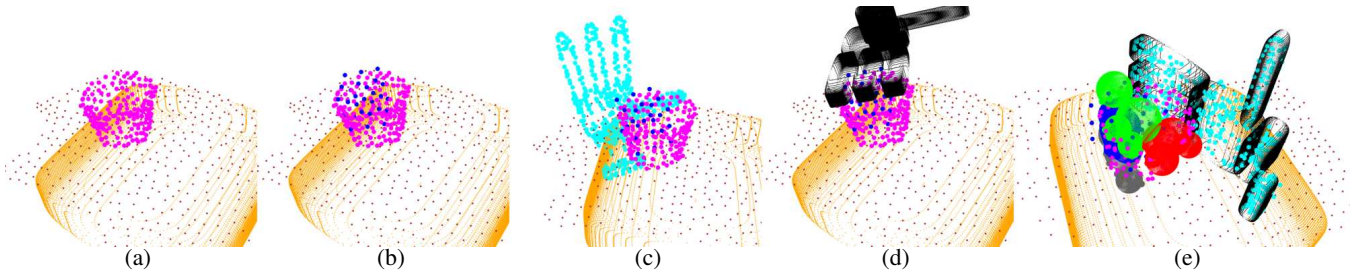

(a) (b) (c) (d) (e)

Fig. 3: Grasping algorithm described in this work. Object downsampled point cloud is shown in Magenta. Blue dots in (b,c) represent object position samples, Allegro hand downsampled cloud shown in Cyan in (c), whereas in (d), gripper special ellipsoid representation is shown in black, best gripper pose in (e) showing the active finger's workspace spheres.

ellipsoid equation, given by:

$$\frac{(x-x_0)^l}{a^l}+\frac{(y-y_0)^l}{b^l}+\frac{(z-z_0)^2}{c^2}=1, \tag{1}$$

where a, b, c are the principal semi axes of the ellipsoid, and x_0, y_0, z_0 denote the offset from origin. As the power l increases, better cuboid approximation is obtained. Equation (1) will be referred to in the sequel for convenience by:

$$EvalSE(\mathcal{E}_o, \mathcal{E}_p, \mathcal{C}, l), \tag{2}$$

where $\mathcal{E}_o$, $\mathcal{E}_p$, $\mathcal{C}$ denote the special ellipsoid offset and semi-principal vectors, and the cloud point(s) whose belonging to the SE parameterized by $\mathcal{E}_o$, $\mathcal{E}_p$ is to be evaluated respectively. These are used to approximate the gripper shape as well as the table as depicted in Fig. 3 and Fig. 4.

B. Object sampling

A complete point cloud is required by our algorithm, this is done during experiments by registering a 3 view point cloud of the object from different view angles. The object cloud is then segmented from the table using random sample consensus (RANSAC) [30], [31]. and both are downsampled (see Fig. 3 (a)). The bounding box of the object is then computed, which is then uniformly sampled into a sampling cloud ${}^o\mathcal{C}_s \in \mathbb{R}^{n_s \times 3}$, with predefined number of sample points n_s, these are visible as blue dots in Fig. 3 (b). A coordinate frame $\mathcal{F}_t$ is assigned to the table point cloud, this is easily done, by assuming the z-axis along the longest dimension, perpendicular to which is the x-axis (same plane), then y-axis is constructed to conclude the frame according to the right hand screw rule. As such the y-axis is always perpendicular to the table plane, along which the table special ellipsoid ${}^t\mathcal{E}_t \in \mathbb{R}^{1\times 6}$ is constructed.

C. Collision check

The algorithm then searches for the best grasping pose, at each iteration, the gripper workspace centroid point (visible as yellow sphere in Fig. 4 (a,b) for allego hand, and franka gripper respectively) is translated to the respective sample point in the sampling cloud $\mathcal{C}_s$. For each of these position samples, several orientation sub-samples, with predefined number n_{os} are then applied and tested, each orientation sub-sample represents a small increment in angle about one axis. An orientation samples of $n_{os} = 64$ means 90^o increments of orientation angle about x, y, and z-axes, thanks to such addition, we no longer require estimation of the object orientation that is usually inaccurate, as well as being meaningless for objects with irregular geometry.

In a first step: for each position/orientation sample pair, the gripper point cloud ${}^t\mathcal{C}_g$ is checked against the table special ellipsoid ${}^t\mathcal{E}_t$ using $EvalSE({}^t\mathcal{E}_{to}, {}^t\mathcal{E}_{tp}, {}^t\mathcal{C}_g, l)$, this is done in the table coordinate frame (as evident by the left superscript) where the table special ellipsoid is defined. If any point of the gripper cloud lies inside the table SE, this means collision with table at this pose sample of the gripper, this is the case shown in Fig. 3 (c). In a second step: for each gripper pose sample, the object point cloud ${}^g\mathcal{C}_o$ is checked against the gripper set of special ellipsoids ${}^g\mathcal{E}_g$ using $EvalSE({}^g\mathcal{E}_{go}, {}^g\mathcal{E}_{gp}, {}^g\mathcal{C}_o, l)$ in the gripper coordinate frame. If any point of the object cloud lies inside any of the gripper SE, this means collision with object at this pose sample of the gripper, this is shown in Fig. 3 (d).

III. Evaluation Metrics

If the gripper pose sample doesn't collide with either the table or the object, then it is considered a grasp pose candidate, to be evaluated against several evaluation metrics and receive a total score, that is in turn compared with that of other pose candidates. The one with highest score is selected for execution. Evaluation metrics used are listed in what follows.

A. Distance to object centroid

The first metric measures how close the gripper workspace centroid point (visible as solid yellow sphere in Fig. 4 (a,b) for allegro hand and franka gripper respectively) to that of the object point cloud (visible as solid cyan sphere in Fig. 4 (a-d)). A higher score is given for gripper pose candidates nearer to the object centroid, computed as:

$$\psi_1 = \frac{1}{d_{oc}+\delta_1}, \tag{3}$$

$$d_{oc} = \sqrt{\left(p^x_{oc}-p^x_{gwc}\right)^2+\left(p^y_{oc}-p^y_{gwc}\right)^2+\left(p^z_{oc}-p^z_{gwc}\right)^2}$$

where ψ_1 is the first metric value, d_{oc} is the Euclidean distance between object centroid point $\boldsymbol{p}_{oc}$ and that of the gripper workspace $\boldsymbol{p}_{gwc}$, and δ_1 is a small positive scalar limiting factor for the maximum values that can be obtained from (3).

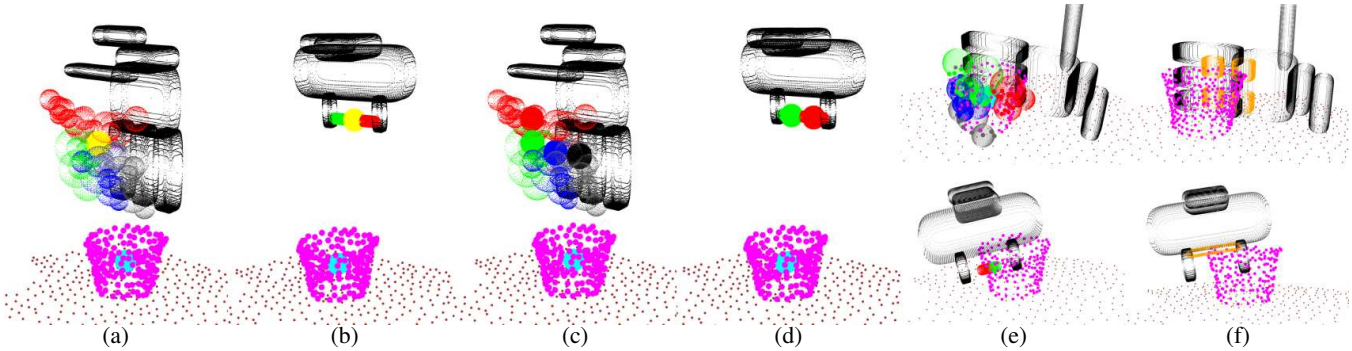

Fig. 4: Grasp pose candidate evaluation metrics. The gripper whole workspace centroid is shown as solid yellow sphere in (a,b). Finger workspace centroid is shown as solid red, green, blue, and black spheres in (c), and as green, red spheres in (d) for the Allegro hand and Franka gripper respectively. Active workspace spheres depicted in (e), while gripper support regions are colored Orange in (f).

B. Object points in workspace spheres

The second metric measures the number of points of the object cloud that reside the workspace spheres of each finger. In contrast to our previous development, where the algorithm forced the selection of grasp poses where at least one point of the object cloud resides in the workspace of each finger, here, we relax this constraint, where an object with smaller size can be grasped without all fingers having access to it. This metric is formulated as:

$$\psi_2 = \sum_f n_o^f * n_{sp}^f, \tag{4}$$

with ψ_2 being the metric value, $f = \{t, i, m, p\}$, $f = \{rf, lf\}$ is the finger index vector for allegro hand and franka gripper (rf and lf for right and left fingers) respectively, n_o^f is the number of points in object cloud accessible to finger f, and n_{sp}^f, the number of active spheres in finger f, these are the ones that has at least one object point inside. The formula in (4) will give more reward for more fingers to have more than one contact solution to the object. The active workspace spheres as well as the object points laying within are shown in Fig. 4 (e) (upper) and Fig. 4 (e) (lower) for the allegro hand and franka gripper respectively.

C. Object points in gripper support regions

This metric gives more reward if more object points are in contact with the gripper base or the palm in case of robotic hand, since this allows for more contact area between the gripper and the object, which in turn results in a more stable grasps. This is implemented as a set of special ellipsoids ${}^g\mathcal{E}_{sr} \in \mathbb{R}^{n_{sr}\times 6}$, designated by "support regions," depicted in Fig. 4 (f) (upper) and Fig. 4 (f) (lower) for allegro hand and franka gripper respectively in orange color, can be formulated as follows:

$$\psi_3 = \sum_{n=1}^{n_{sr}} n_o^{(n)} + \xi, \tag{5}$$

where ψ_3 is the metric value, $n_o^{(n)}$ is the number of object cloud points residing in support region n, this is evaluated using (1) as $EvalSE({}^g\mathcal{E}_{sro}, {}^g\mathcal{E}_{srp}, {}^g\mathcal{C}_o, l)$, while ξ is the multi-support region reward factor, computed using Algorithm 1. In (5) we can observe, higher reward is obtained for gripper poses where multiple support regions are in contact with object, this can be very useful in finding poses that fulfill local geometric similarity.

Algorithm 1: Multi-support region reward algorithm

```
i = 0
for each support region n in n_sr do
    if n_o^(n) then
        i = i + 1
    end if
end for
ξ = i^i
```

D. Object centroid encapsulation

The fourth metric encourages gripper poses that maintain symmetry between the object and gripper workspace in case of multi-DoF hands, where the object centroid point is required to be positioned between the thumb workspace spheres centroid (solid red sphere in Fig. 4 (c)) and those of the index, middle and pinky fingers (solid green, blue, and black spheres respectively in the same figure). This is achieved along the z-axis in the gripper frame, as well as pushing for poses close to the palm of the hand, by giving more reward for poses moving along x-axis in the gripper frame.

$$\psi_4 = \begin{cases} 1, & \text{if } cond\#1 \\ 2, & \text{if } cond\#1 \wedge cond\#2 \\ 0, & \text{if } otherwise \end{cases}. \tag{6}$$

$$\begin{aligned} cond\#1 : & \; p_{oc}^z > p_{twc}^z \wedge p_{oc}^z < p_{iwc}^z \\ & \wedge p_{oc}^z < p_{mwc}^z \wedge p_{oc}^z < p_{pwc}^z, \\ cond\#2 : & \; p_{oc}^x \leq p_{twc}^x \wedge p_{oc}^x \leq p_{iwc}^x \\ & \wedge p_{oc}^x \leq p_{mwc}^x \wedge p_{oc}^x \leq p_{pwc}^x, \end{aligned}$$

where ψ_4 is the fourth metric value, $\boldsymbol{p}_{twc}$, $\boldsymbol{p}_{iwc}$, $\boldsymbol{p}_{mwc}$, and $\boldsymbol{p}_{pwc}$ denote the thumb, index, middle, and pinky workspace centroid points respectively. The same metric formula is

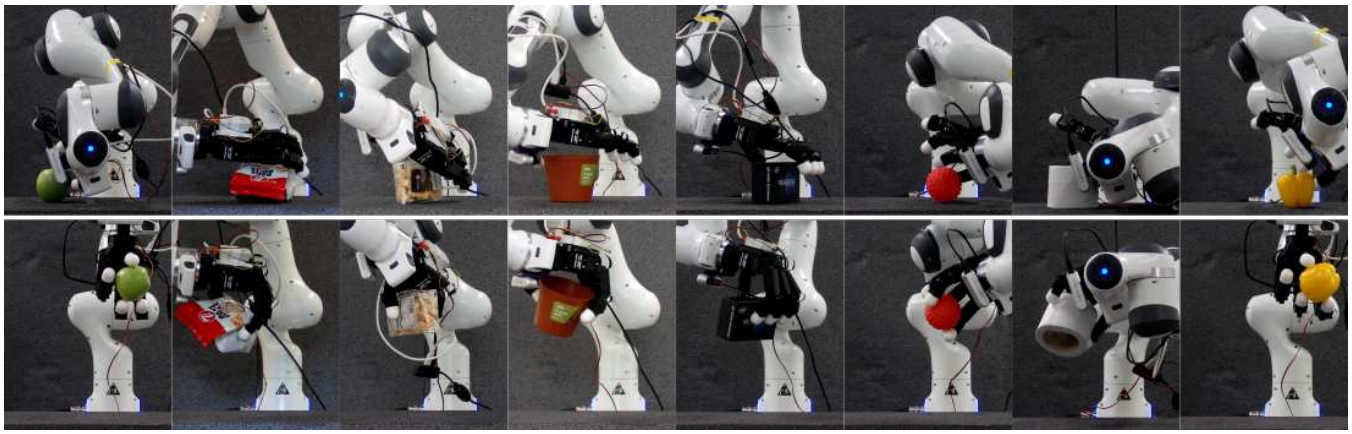

Fig. 5: Screenshots from allegro hand grasping experiments, featuring the objects: yellow pepper, toilet paper roll, soft ball, realsense box, plant pot, croutons and bake rolls packages, apple in order from right to left. Upper screenshots show the pre-grasp pose output of the algorithm, while the lower show the objects after the execution of a successful grasp.

applied to the 2 fingered franka gripper, with only the thumb and index fingers active. Finally, the total metric score ψ is evaluated as follows:

$$\psi = \sum_{i=1}^{4} \lambda_i \psi_i, \tag{7}$$

where $\lambda_{1...4}$ denote positive scalar values to provide different weights for the corresponding metrics.

IV. Experiments

In this section, the experimental results of the enhanced grasping algorithm are presented and discussed, using the system parameters provided in Table I. Two sets of experiments have been performed, one per gripper type. Each gripper was mounted to the Franka Emika arm (7 DoF), controlled in real-time with Franka control interface. The communication between the robot controller, the realsense camera, and the grippers is done through ROS. Motion planning is achieved using MoveIt! [32] based on the pose targets generated by our algorithm. The algorithm is written in C++, running on standard labtop with 8th generation core i7 processor with no GPU.

Experiments feature 20 objects to be grasped with both the Allegro right hand, and the Franka 2 finger gripper, the objects we selected such that they are within the grasping volume of each gripper while maintaining considerable variation in size/shape/texture. An almost complete point cloud of the object is constructed from 3 view points using the Intel RealSense-D435 depth camera [33], then the grasping algorithm computes a grasping pose based on the generated point cloud as well as the gripper model to be used. The arm moves to this pose at an approach distance of 10 cm in z-axis, the gripper then approaches the object before performing the grasping action. The grasping action used in both grippers is a simple position control to a closed fingers configuration. To conclude each experiment, the arm moves upward for 20 cm. An object is marked as grasped if it remains in static condition inside the gripper for more than 10 seconds.

A sample of the objects used in experiments is shown in Fig. 6, screenshots of which in the pre-grasp pose generated by the algorithm as well as after being grasped for the Allegro right hand is shown in Fig. 5 (upper), Fig. 5 (lower) respectively. Screenshots for the same objects being grasped by the Franka gripper are shown in Fig. 7 (upper), Fig. 7 (lower) as well.

TABLE I: Grasping algorithm parameters

Parameter	Allegro Hand	Franka Gripper
n_e (special ellipsoids)	7	5
n_s (position samples)	1000	1000
n_f (fingers)	4	2
n_{sp} (workspace spheres)	10	10
n_g (gripper cloud size in points)	500	500
n_o (object cloud size in points)	≤ 500	≤ 500
n_{os} (orientation samples)	5832	64
n_{sr} (support regions)	4	2
λ_1 (metric#1 weight)	1000	1000
δ_1 (metric#1 limiting factor)	10^{-5}	10^{-5}
λ_2 (metric#2 weight)	1.0	1.0
λ_3 (metric#3 weight)	1000	1000
λ_4 (metric#4 weight)	2000	2000

A. Discussion

The results of the experiments conducted is provided in Table II for both gripper types, with average success rates of

Fig. 6: The set of objects used in evaluating the grasping algorithm.

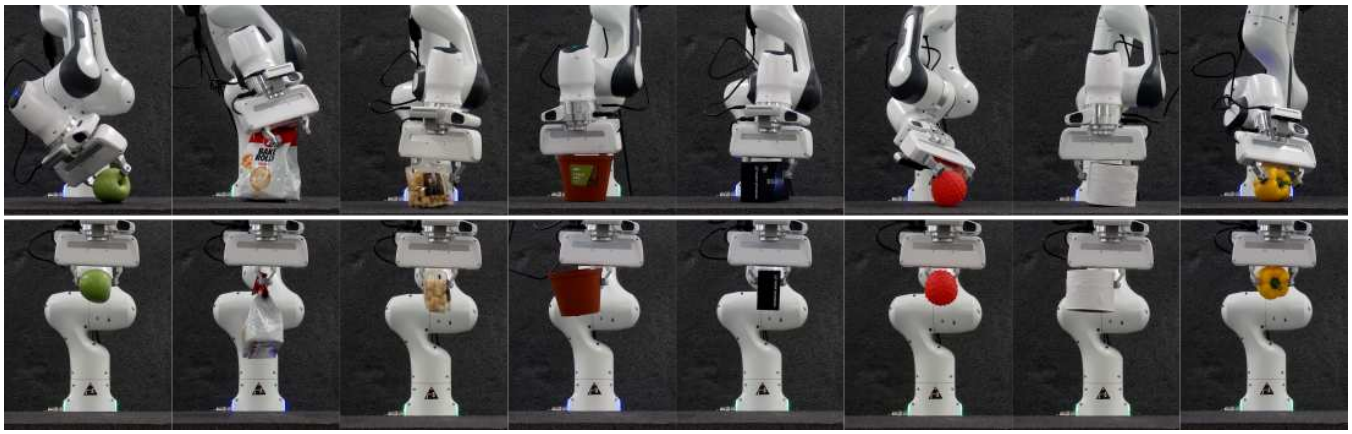

Fig. 7: Screenshots from franka gripper grasping experiments featuring the same objects in Fig. 5.

76% and 85.5% for the Allegro hand and Franka gripper respectively. The results show the positive impact of the improved evaluation metrics and more importantly the effect of using higher sampling in the quest for the most successful grasp pose as compared to the results reported in [29]. The downside is indeed the computation time, that can range from 5 to 15 minutes, depending on the object cloud size as well as the gripper type. In Table II, we can see that our algorithm is capable of grasping rigid/deformable objects like bake rolls, croutons and cookies packages, these are inherently rigid objects but packed in loose packaging material thanks to adopting "closure till force balance" grasp policy.

It can be observed that the Allegro hand has higher grasp success rates for bulky objects, although very good grasp poses are generated for small objects as well. This happens due the fact that simple finger closure to a predefined positions is limiting its capabilities and won't be suitable for all object sizes. Also increasing the force applied per finger to obtain more stable grasps, requires higher value for position control gains which results in oscillations in the thumb configuration, that can sometimes displace the object, resulting in failures. This is visible in the video submitted with this paper. The Franka gripper showed high grasping success rates for most of the objects except for the "Mug" where the algorithm generated grasp poses for the mug handle, given the low friction material of the gripper along with the torque generated (due to mug's weight) while grasping from such location, grasp failure was the outcome.

TABLE II: Grasp success rate per gripper for different objects

Object	Characteristic	A. Hand	F. Gripper
Storage bin	rigid	70%	80%
Tooth paste	rigid deformable	30%	100%
Dish brush	rigid deformable	0%	100%
Plant pot	rigid deformable	100%	80%
Handless cup	rigid	90%	60%
Toilet paper roll	soft	90%	90%
Realsense box	rigid	100%	100%
Air duster	rigid	60%	70%
Apple (large)	rigid	90%	80%
Banana (medium)	soft	20%	100%
Cereals box	rigid deformable	70%	100%
Coffee jar	rigid	80%	90%
Mug	rigid	70%	0%
Sand bucket	rigid deformable	90%	100%
Cookies package	rigid deformable	90%	100%
Bake rolls	rigid deformable	90%	80%
Pepper (yellow)	soft	100%	100%
Croutons pack	rigid deformable	100%	100%
Soft ball toy	soft	90%	80%
Ketchup bottle	soft	90%	100%
Average		76%	85.5%

B. Future Work

Following the successful validation of the impact of high sampling on grasp success rate, the authors would like to explore even higher sampling, with future goals of implementing a deep convolution neural network to act as a function approximator for the development in hand. The input to which is the object point cloud as well as the gripper type, with the grasp pose serving as the output. As such, once tuned, the network would solve the problem of large computation time. Once the grasp success rate of the grasping algorithm reaches 95%, we plan to generate automatically training data from simulation.

In order to leverage the true potential of our algorithm with high DoF hands, extensions must be added for planning grasp points on objects. This is hardly needed for simple jaw grippers, and as such was avoided to maintain algorithm generality, an action the authors plan to withdraw in future work.

V. Conclusion

In this work, successful enhancement to the novel grasping algorithm based on finger workspace spheres has been presented. Positive impact in terms of grasp success rate has been reported, being applied to a complex hand with 16 DoF as well as a simple jaw gripper with 2 DoF, maintaining the algorithm versatility. Successful experiments have shown better results with the newly proposed grasp candidate evaluation metrics and higher sampling in terms of candidate position and orientation.

ACKNOWLEDGMENTS

This work is funded by EPSRC under grant agreement EP/R02572X/1, UK National Center for Nuclear Robotics initiative (NCNR).

REFERENCES

[1] S. Jain and B. Argall, "Grasp detection for assistive robotic manipulation," in *2016 IEEE International Conference on Robotics and Automation (ICRA)*, May 2016, pp. 2015–2021.

[2] A. T. Miller, S. Knoop, H. I. Christensen, and P. K. Allen, "Automatic grasp planning using shape primitives," in *2003 IEEE International Conference on Robotics and Automation (ICRA)*, Sep. 2003, pp. 1824–1829 vol.2.

[3] V. Lippiello, F. Ruggiero, B. Siciliano, and L. Villani, "Visual grasp planning for unknown objects using a multifingered robotic hand," *IEEE/ASME Transactions on Mechatronics*, vol. 18, no. 3, pp. 1050–1059, June 2013.

[4] J. Baumgartl and D. Henrich, "Fast vision-based grasp and delivery planning for unknown objects," in *ROBOTIK 2012; 7th German Conference on Robotics*, May 2012, pp. 1–5.

[5] J. Bohg, A. Morales, T. Asfour, and D. Kragic, "Data-driven grasp synthesis ;a survey," *IEEE Transactions on Robotics*, vol. 30, no. 2, pp. 289–309, April 2014.

[6] D. Kappler, J. Bohg, and S. Schaal, "Leveraging big data for grasp planning," in *2015 IEEE International Conference on Robotics and Automation (ICRA)*, May 2015, pp. 4304–4311.

[7] A. ten Pas, M. Gualtieri, K. Saenko, and R. Platt, "Grasp pose detection in point clouds," *The International Journal of Robotics Research*, vol. 36, no. 13-14, pp. 1455–1473, 2017.

[8] Z. Abderrahmane, G. Ganesh, A. Crosnier, and A. Cherubini, "Haptic zero-shot learning: Recognition of objects never touched before," *Robotics and Autonomous Systems*, vol. 105, pp. 11 – 25, 2018.

[9] Z. Abderrahmane, G. Ganesh, A. Crosnier, and A. Cherubini, "A deep learning framework for tactile recognition of known as well as novel objects," *IEEE Transactions on Industrial Informatics*, vol. 16, no. 1, pp. 423–432, Jan 2020.

[10] J. K. Salisbury, J. K., "Kinematic and force analysis of articulated mechanical hands," *Journal of Mechanisms, Transmissions, and Automation in Design*, vol. 105, no. 1, pp. 35–41, 1983.

[11] V.-D. Nguyen, "Constructing force closure grasps," *The International Journal of Robotics Research*, vol. 7, no. 3, pp. 3–16, 1988.

[12] C. Ferrari and J. Canny, "Planning optimal grasps," in *Proceedings 1992 IEEE International Conference on Robotics and Automation*, May 1992, pp. 2290–2295.

[13] R. M. Murray, S. S. Sastry, and L. Zexiang, *A Mathematical Introduction to Robotic Manipulation*, 1st ed. Boca Raton, FL, USA: CRC Press, Inc., 1994.

[14] J. Mahler, J. Liang, S. Niyaz, M. Aubry, M. Laskey, R. Doan, X. Liu, J. A. Ojea, and K. Goldberg, "Dex-Net 2.0: Deep Learning to Plan Robust Grasps with Synthetic Point Clouds and Analytic Grasp Metrics," May 2018, to appear at Robotics: Science and Systems 2017. [Online]. Available: https://hal.archives-ouvertes.fr/hal-01801048

[15] Q. Lei, J. Meijer, and M. Wisse, "Fast c-shape grasping for unknown objects," in *2017 IEEE International Conference on Advanced Intelligent Mechatronics (AIM)*, July 2017, pp. 509–516.

[16] K. Huebner and D. Kragic, "Selection of robot pre-grasps using box-based shape approximation," in *2008 IEEE/RSJ International Conference on Intelligent Robots and Systems (IROS)*, Sep. 2008, pp. 1765–1770.

[17] M. Przybylski, T. Asfour, and R. Dillmann, "Unions of balls for shape approximation in robot grasping," in *2010 IEEE/RSJ International Conference on Intelligent Robots and Systems (IROS)*, Oct 2010, pp. 1592–1599.

[18] B. S. Zapata-Impata, "Using geometry to detect grasping points on 3d unknown point cloud," in *Proceedings of the 14th International Conference on Informatics in Control, Automation and Robotics (ICINCO)*. SciTePress, 2017, pp. 154–161.

[19] A. H. Quispe, B. Milville, M. A. Gutiérrez, C. Erdogan, M. Stilman, H. Christensen, and H. B. Amor, "Exploiting symmetries and extrusions for grasping household objects," in *2015 IEEE International Conference on Robotics and Automation (ICRA)*, May 2015, pp. 3702–3708.

[20] Q. Lei and M. Wisse, "Fast grasping of unknown objects using force balance optimization," in *2014 IEEE/RSJ International Conference on Intelligent Robots and Systems (IROS)*, Sep. 2014, pp. 2454–2460.

[21] Q. Lei, J. Meijer, and M. Wisse, "A survey of unknown object grasping and our fast grasping algorithm-c shape grasping," in *2017 3rd International Conference on Control, Automation and Robotics (ICCAR)*, April 2017, pp. 150–157.

[22] T. Suzuki and T. Oka, "Grasping of unknown objects on a planar surface using a single depth image," in *2016 IEEE International Conference on Advanced Intelligent Mechatronics (AIM)*, July 2016, pp. 572–577.

[23] Y. Lin, S. Wei, and L. Fu, "Grasping unknown objects using depth gradient feature with eye-in-hand rgb-d sensor," in *2014 IEEE International Conference on Automation Science and Engineering (CASE)*, Aug 2014, pp. 1258–1263.

[24] M. Adjigble, N. Marturi, V. Ortenzi, V. Rajasekaran, P. Corke, and R. Stolkin, "Model-free and learning-free grasping by local contact moment matching," in *2018 IEEE/RSJ International Conference on Intelligent Robots and Systems (IROS)*, Oct 2018, pp. 2933–2940.

[25] C. Eppner and O. Brock, "Grasping unknown objects by exploiting shape adaptability and environmental constraints," in *2013 IEEE/RSJ International Conference on Intelligent Robots and Systems (IROS)*, Nov 2013, pp. 4000–4006.

[26] I. Lenz, H. Lee, and A. Saxena, "Deep learning for detecting robotic grasps," *The International Journal of Robotics Research*, vol. 34, no. 4-5, pp. 705–724, 2015.

[27] D. Fischinger, A. Weiss, and M. Vincze, "Learning grasps with topographic features," *The International Journal of Robotics Research*, vol. 34, no. 9, pp. 1167–1194, 2015.

[28] B. S. Zapata-Impata, P. Gil, J. Pomares, and F. Torres, "Fast geometry-based computation of grasping points on three-dimensional point clouds," *International Journal of Advanced Robotic Systems*, vol. 16, no. 1, pp. 1–18, 2019.

[29] M. Sorour, K. Elgeneidy, A. Srinivasan, M. Hanheide, and G. Neumann, "Grasping unknown objects based on gripper workspace spheres," in *2019 IEEE/RSJ International Conference on Intelligent Robots and Systems (IROS)*, Nov 2019, pp. 1541–1547.

[30] R. B. Rusu, "Semantic 3d object maps for everyday manipulation in human living environments," Ph.D. dissertation, Computer Science department, Technische Universitaet Muenchen, Germany, October 2009.

[31] R. B. Rusu and S. Cousins, "3D is here: Point Cloud Library (PCL)," in *IEEE International Conference on Robotics and Automation (ICRA)*, Shanghai, China, May 9-13 2011.

[32] I. A. Sucan and S. Chitta, "Moveit!" [Online] Available: http://moveit.ros.org.

[33] Intel.com, "Intel realsense depth camera," https://click.intel.com/intelr-realsensetm-depth-camera-d435.html.